"Prediction of flash-flood hazard impact from Himalayan river profiles"

AGU PUBLICATIONS

Geophysical Research Letters

RESEARCH LETTER
10.1002/2015GL063784

Key Points:
- We analyzed geomorphic impact of 2013 flash floods in the NW Himalaya
- We concluded that flood hazard impact is predictable through channel steepness
- We also analyzed river response throughout its length during flash flood

Supporting Information:
- Texts S1 and S2 and Figures S1 and S2

Correspondence to:
R. Devrani,
rahuldevrani18@gmail.com

Citation:
Devrani, R., V. Singh, S. M. Mudd, and H. D. Sinclair (2015), Prediction of flash flood hazard impact from Himalayan river profiles, *Geophys. Res. Lett.*, *42*, 5888–5894, doi:10.1002/2015GL063784.

Received 18 APR 2015
Accepted 30 JUN 2015
Accepted article online 1 JUL 2015
Published online 28 JUL 2015

Prediction of flash flood hazard impact from Himalayan river profiles

R. Devrani[1], V. Singh[1], S. M. Mudd[2], and H. D. Sinclair[2]

[1]Department of Geology, University of Delhi, New Delhi, India, [2]School of Geosciences, University of Edinburgh, Edinburgh, UK

Abstract To what extent can we treat topographic metrics such as river long profiles as a long-term record of multiple extreme geomorphic events and hence use them for hazard prediction? We demonstrate that in an area of rapid mountain erosion where the landscape is highly reactive to extreme events, channel steepness measured by integrating area over upstream distance (chi analysis) can be used as an indicator of geomorphic change during flash floods. We compare normalized channel steepness to the impact of devastating floods in the upper Ganga Basin in Uttarakhand, northern India, in June 2013. The pattern of sediment accumulation and erosion is broadly predictable from the distribution of normalized channel steepness; in reaches of high steepness, channel lowering up to 5 m undercut buildings causing collapse; in low steepness reaches, channels aggraded up to 30 m and widened causing flooding and burial by sediment. Normalized channel steepness provides a first-order prediction of the signal of geomorphic change during extreme flood events. Sediment aggradation in lower gradient reaches is a predictable characteristic of floods with a proportion of discharge fed by point sources such as glacial lakes.

1. Introduction

The application of topographic analysis in determining tectonic forcing of landscapes at timescales that bridge the historical ($<10^2$ years) and geological ($>10^6$ years) is improving assessment of seismic hazard [*Kirby et al.*, 2008]. Assuming the long-term erosion of rivers in mountain belts can be modeled as a power law function of channel slope versus water discharge (approximated by upstream catchment area [*Whipple and Tucker*, 1999]), the progressive reduction of channel gradient with upstream area is predictable [*Hack*, 1960]. However, in the Himalaya, the long profiles of rivers do not decline from their mountain sources asymptotically to the Gangetic Plains but instead exhibit downstream steepening over active fault structures such as the Main Central Thrust [*Seeber and Gornitz*, 1983]. Quantification of the degree of steepening has enabled differential rock uplift fields and their associated fault structures to be identified in a range of settings [*Kirby and Whipple*, 2012] with some of the earliest applications in the Himalaya [e.g., *Hodges et al.*, 2004].

Increases in channel gradients via, for example, tectonic forcing will increase unit stream power resulting in higher incision rates. This provides a mechanism by which rivers adjust toward a dynamic steady state between rock uplift and river incision. In rivers where the channel is bound by bedrock surfaces, incision is said to be detachment limited; i.e., changes in channel geometry can only occur due to detachment of rock from the channel boundary [*Howard*, 1994]. In contrast, where sediment flux exceeds the transport capacity of a river, the system becomes transport limited whereby the river long profile is dictated by the downstream divergence of sediment flux [*Whipple and Tucker*, 2002]. In this case, the volumetric transport capacity is a power function of unit stream power [*Willgoose et al.*, 1991]. Therefore, as channel gradients decrease (normalized for drainage area), so sediment transport capacity of the river declines and sedimentation is enhanced. However, this transition from bedrock incision into channel alluviation is also a function of grain size and sediment supply rate [*Sklar and Dietrich*, 1998].

Although channel steepness, normalized for drainage area, has been demonstrated as a proxy for long-term erosion rates [e.g., *Kirby and Whipple*, 2012], to our knowledge it has not been used as a predictor of the spatial distribution of channel incision during extreme events. Here we exploit a major event which occurred on 16 and 17 June 2013, which devastated the Mandakini River Valley in the upper Ganga basin [*Ziegler et al.*, 2014]; heavy rainfall in the region was augmented by the breaching of a lake on the edge of the Chorabari glacier that enhanced the flood discharge [*Dobhal et al.*, 2013]. Our goal is to determine if the spatial pattern of channel steepness prior to the flooding event in 2013 was consistent with topographic modification along the Mandakini River that occurred during the event.

2. Methodology

Our topographic analysis of river long profiles in the Mandakini basin normalizes for drainage area by integrating drainage area over flow distance. This method, first suggested by *Royden et al*. [2000], produces a transformed coordinate, χ (chi), which has dimensions of length [*Perron and Royden*, 2013]. The elevation of the channel can then be plotted against the χ coordinate, and the gradient of the transformed profile in χ elevation space (which we call M_χ) provides a metric that can be used to compare channel segments with different drainage areas.

The chi method is underpinned by the stream power model of channel incision [*Perron and Royden*, 2013]. It applies to bedrock rivers; these may have thin alluvial covering but are defined as rivers where bedrock must be incised in either the bed or banks for the river to change its form [cf. *Hancock et al*., 1998]; we choose this model because field observations indicate that the Mandakini River was predominantly bedrock prior to the event. This model is an imperfect description of channel incision [e.g., *Lague*, 2014], and other models have been proposed, including those that incorporate the role of sediment supply [*Sklar and Dietrich*, 1998] and erosion thresholds [*Snyder et al*., 2003].

However, even if the stream power incision model is an imperfect description of channel incision, M_χ can still be calculated and allows at least a qualitative comparison of the steepness of channel segments relative to their upstream area, from different parts of the channel network. Analytical solutions of the stream power model suggest that M_χ will reflect channel erosion even if different segments of the channels are eroding at different rates [*Royden and Perron*, 2013]; this prediction has been corroborated with comparison to field data [*Perron and Royden*, 2013; *Mudd et al*., 2014]. The normalized steepness M_χ is related to the normalized steepness index, k_{sn} (see Text S1 in the supporting information), which has been used as a proxy for both erosion rates [e.g., *Ouimet et al*., 2009] and tectonic signals [e.g., *Kirby and Whipple*, 2012] in the Himalayas. Both chi analysis and the normalized steepness index (k_{sn}) have been found to correlate well with erosion rates in the nearby Yamuna River which is the basin immediately to the west of the Ganga [*Scherler et al*., 2014]. We have followed methodology by *Mudd et al*. [2014] to extract χ (chi) and M_χ (Text S1 in the supporting information).

3. Results

3.1. Topographic Analysis of the Mandakini Basin

We focus on the westernmost of the Mandakini upper tributaries; this tributary drains the valley containing the Kedarnath temple and comprises three distinct reaches (Figures 2b and 3a) (see Text S2 in the supporting information). The upper reach has a low-gradient main channel with extensive moraines and glaciers in its headwaters; the M_χ value is relatively low ($M_\chi \sim 3$) (Figures 2b and 3a). Approximately 1 km south of Kedarnath, the river channel steepens downstream and the valley narrows over a distance of around 7 km with M_χ values significantly greater (>150%) than the upper reaches ($M_\chi \sim 7.9$) (Figures 2a, 2b, and 3a); this middle reach has gneisses and schists over more granitic rocks in the hanging wall of the Main Central Thrust [*Valdiya et al*., 1999]. Values of M_χ decrease (~4.5) again downstream above the town of Gaurikund (at ~ 6 km in Figure 3a), and the valley also widens from this point.

3.2. Impact of Flash Floods

On 16 and 17 June 2013, following sustained heavy rainfall, a series of flash floods caused devastation down the Mandakini Valley and south to the exit of the Ganga from the mountain front near Rishikesh and Haridwar killing approximately 5700 people. Hillslope runoff combined with a lake outburst at the head of the Chorabari glacier caused the remobilization of glacial moraine, hillslope debris, and valley alluvium as debris and mud flows [*Dobhal et al*., 2013]. The sediment-laden waters devastated infrastructure in two ways, either by burying buildings (aggradation) or by incising and undercutting foundations as the active channel, predominantly composed of either bedrock or moraine material, which responds to incision in detachment limited manner [e.g., *Hobley et al*., 2011], widened (see Figure S1 in the supporting information). The distribution of sediment aggradation and bedrock incision has been mapped through field observations and repeat satellite imagery in Kedarnath Valley (Figure S1 in the supporting information).

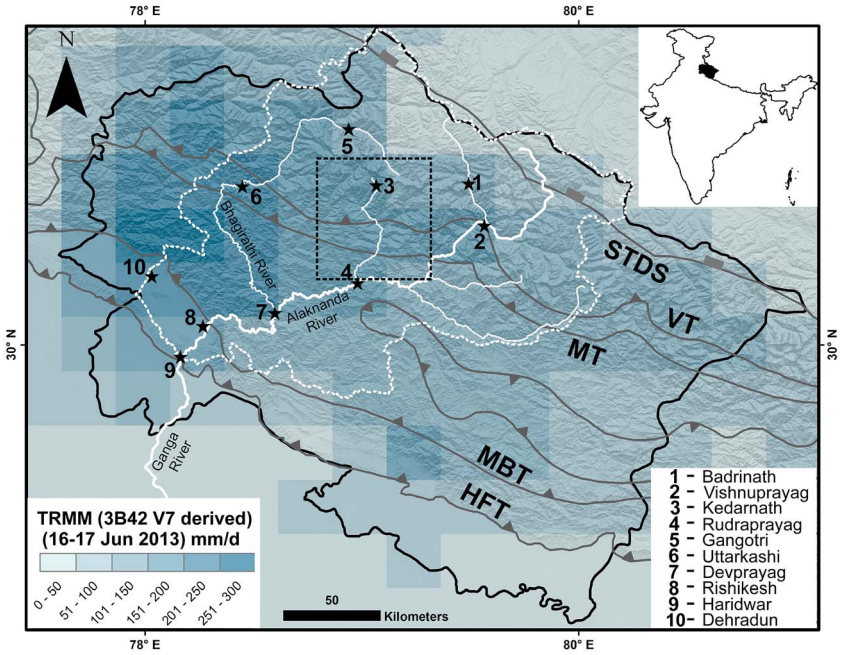

Figure 1. Daily Tropical Rainfall Measuring Mission (TRMM) (3B42 V7 derived) data draped over shaded relief map of northwest Himalaya. The black color boundary represents Uttrakhand (India), and dotted white color boundary is showing Ganga River basin (above Himalayan Frontal Thrust (HFT)). Black dotted box shows location in Figure 2a; white lines represent major tributaries of the Ganga River. The fault locations are after *Valdiya et al.* [1999] and *Bickle et al.* [2001]; STDS: South Tibetan detachment system, VT: Vaikrita thrust, MT: Munsiari thrust, MBT: Main Boundary thrust, and HFT: Himalayan Frontal Thrust.

3.2.1. Kedarnath Valley

In the uppermost reaches around the Kedarnath Temple (Figures 1, 2b, and 3a), sediment that had been released from the upstream erosion of glacial moraine accumulated where the active valley widened around Kedarnath from ~ 250 m to ~ 370 m wide (Figure S1 in the supporting information). Boulders up to 12 m accumulated upstream of the temple, protecting it from much of the surge. In the streets of Kedarnath, an average aggradation of 2.5 m of boulders, gravel, and finer sediment has been observed (Figure 3c).

Downstream of Kedarnath, where the river channel steepens, previously accumulated alluvial channel fill was stripped away by the floods. The active channel width increased from approximately 30 m to 120 m causing lateral undercutting bedrock bounded hillslopes and the complete obliteration and removal of settlements such as the village of Rambara (Figures 3e and S1 in the supporting information). Incision in the valley of at least 8 m is observed in this reach of the river channel incision continued for approximately 7 km downstream throughout the reach of highest M_χ values (~7.9) (Figures 2a and 3e).

Approximately 11 km downstream of Kedarnath, at the village of Gaurikund, sediment aggradation once again dominates with up to 5 m of sediment filling the streets of the village. Farther downstream where the river turns eastward and the valley widens, approximately 10 m of sediment accumulated near Sonprayag (Figures 3a and 3g).

In summary, the impact of the flash flood in the Kedarnath Valley comprised an upper reach characterized by low M_χ values (~3) and the aggradation of coarse debris across the valley floor. In the middle reach, where channel gradients and M_χ values increased (~7.9), the channel incised and widened through undercutting. In the lower reach where M_χ values decreased (~4.5) and the valley widened, sediment aggradation once again dominated.

3.2.2. Neighboring Valleys

Access to the lower Kaliganga and Madhyamaheshwar Valleys (Figure 2a) enabled documentation of the flood impact south of the Main Central Thrust (MCT), but access was restricted to the north due to catastrophic damage to transport infrastructure and a military-led reconstruction and humanitarian effort.

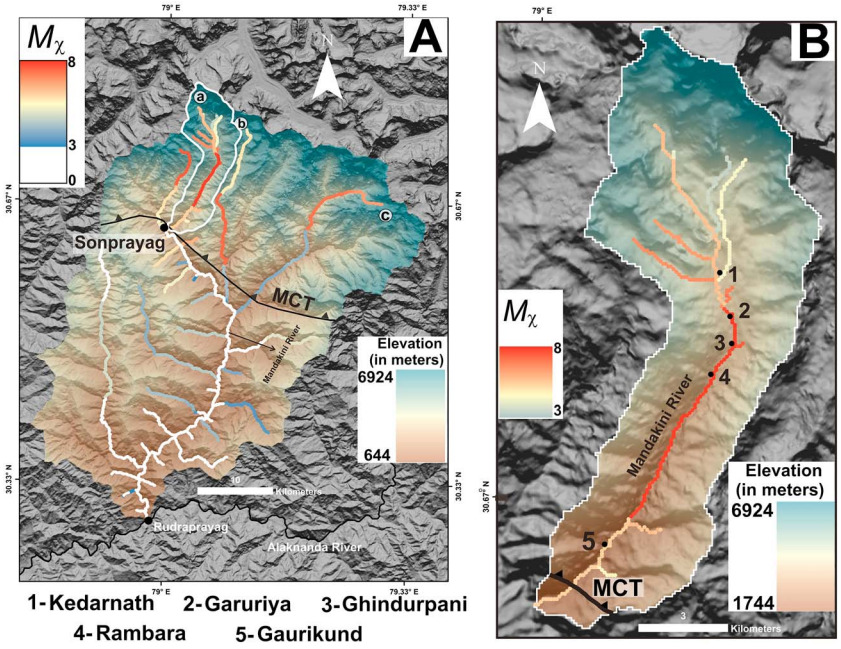

Figure 2. (a) Shaded relief map (30 m Advanced Spaceborne Thermal Emission and Reflection digital elevation model (ASTER DEM)) of the Mandakini River basin, showing plan view of color-coded chi values within Mandakini River basin. a: Mandakini River, b: Kaliganga River, and c: Madhyamaheshwar-Ganga River. (b) Topographic map (30 m ASTER DEM) draped over the shaded relief map of the Kedarnath Valley, showing plan view of color-coded chi values and highly impacted township in Kedarnath Valley.

Around the MCT, the Kaliganga River shows relatively low M_χ values (~3.4) from its upstream reach and the signal of channel modification is dominated by lateral erosion and undercutting of the local hillslopes driving rockslides and debris flows (see Figure S2a, S2b, and S2c in the supporting information). Downstream from this point, the Kaliganga joins the Mandakini and M_χ values are reduced ($M_\chi \sim 2.2$) relative to the Kaliganga upstream of the Mandakini junction ($M_\chi \sim 3.2$). In this reach, the channel comprises large 3–4 m high bars with a wavelength of 10 m composed primarily of large (>1 m) boulders (Figure S2d in the supporting information). The neighboring Madhyamaheshwar-Ganga drains from the northwest and downstream from the MCT comprises a low-gradient reach with low M_χ values ($M_\chi \sim 3.2$; similar to those downstream of the Kaliganga and Mandakini junction) that is retained as it merges with the Mandakini (Figure S2a, S2b, and S2c in the supporting information). Throughout this region, channel modification is characterized by the accumulation of thick, boulder-dominated bar forms that have aggraded by 4–5 m, causing burial of many of the isolated buildings in the channel (Figure S2h in the supporting information). Overall, from these two neighboring valleys there is a signal where high M_χ values are characterized by channel incision and undercutting of hillslopes, and at lower values, sediment aggradation of thick bar forms dominate.

4. Discussion and Conclusion

4.1. Discussion

In this example from the western Himalaya, we have explored whether the first-order geomorphic characteristics of the long river profile which are accessible from digital topography can be interpreted as an integrated record of extreme storm events. Estimation for paleoflood deposits in the Alaknanda Valley suggests a mean 55 years repeat interval [*Wasson et al.*, 2013]. However, the erosive record of a circa 13 ka glacial deposit near Rambara indicates that the 2013 floods were the largest since the glacial maxima in the upper Kedarnath Valley.

The results suggest that chi analysis of river channel steepness, via the chi gradient M_χ [*Royden et al.*, 2000; *Perron and Royden*, 2013; *Mudd et al.*, 2014], provides a potentially important methodology for assessing the long-term trajectory of geomorphic change driven by extreme events. In order to relate the chi analysis to the geomorphic signal of this event, we must integrate the spatial pattern of incision and

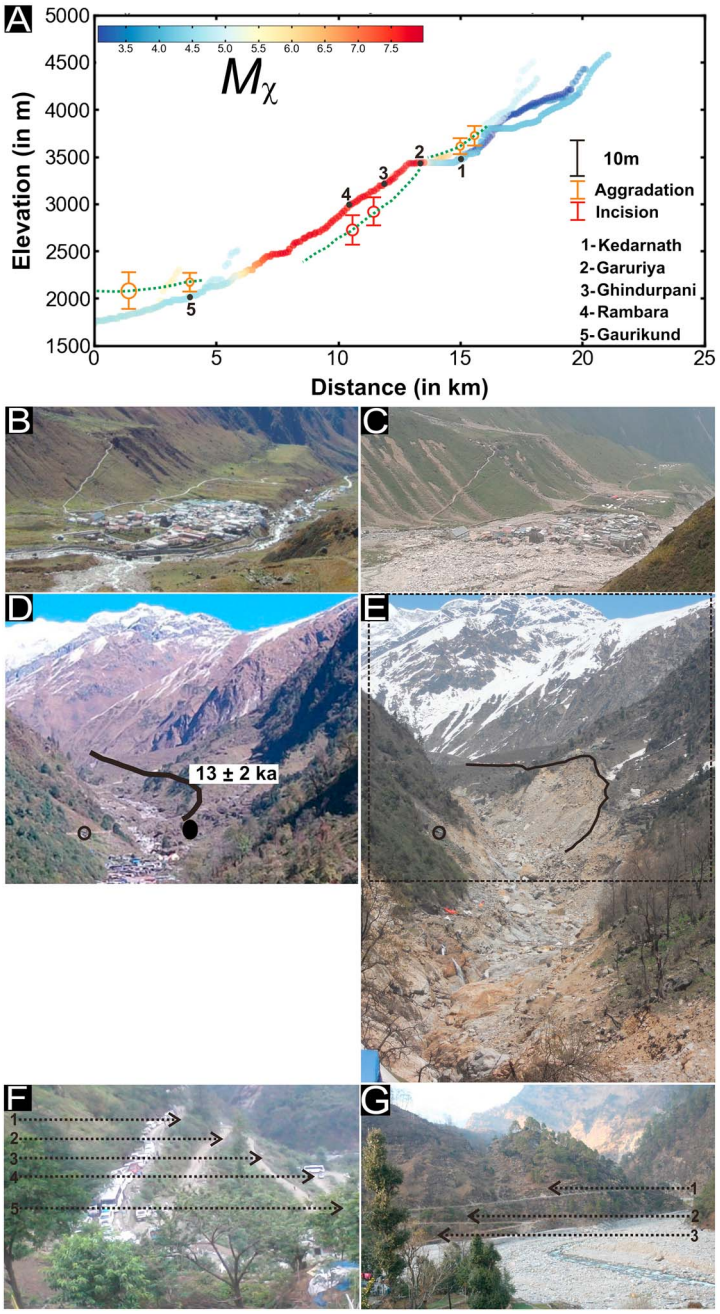

Figure 3. (a) Longitudinal profile of Mandakini River and its tributaries (in the Kedarnath Valley, for location see Figure 2a) color coded by chi values, also showing different geomorphic processes zones on the long profile of the Mandakini River. The A_0 is 1000 m^2, and relative *m/n* value is 0.35 (see supporting information for details). Circles with error bars indicate localities where preevent and postevent changes in the channel elevation can be quantified (with error bars). Dashed green line indicates where these localities can be laterally traced using satellite data (given source such as Google Earth data). (b) Preevent view of the Kedarnath town, note the free accommodation space near the Kedarnath temple (c) Preevent view of the Kedarnath town; photograph also shows extensive aggradation along the Kedarnath town (photo courtesy: Konark). (d) Preevent photograph of the Rambara; note the extension of lateral moraine in Kedarnath Valley ~ 13 ka (Modified after *Mehta et al.* [2012]). (e) Postevent photograph of the upstream and downstream of the Rambara suggests an extreme landscape incision, (see back circle for landmark location in Figures 3d and 3e). Also note the flushing of the glacial sediments from the Rambara. (f) Preevent photograph near road bend of the National Highway109 near Sitapur (~300 m downstream Sonprayag, for location refer to Figure2a) (photo courtesy: Dr. Navin Juyal). (g) Postevent photograph near Sitapur; note that in the filling of the Mandakini River up to two levels the road bends on the National Highway 109 (photo courtesy: Dr. Navin Juyal).

aggradation along with the channel widening and the evidence of a point source for some of the discharge. Embedded within chi analysis is an assumption that channel incision is a function of the discharge divided by the width of the channel; the final form of the stream power law combines an assumption that discharge, Q, is a function of drainage area ($Q = k_Q A^a$) and channel width, w, is also a function of drainage area ($w = k_w A^b$). The m exponent therefore combines the exponents a and b ($m = a - b$). The exponent b is positive and less than 1 [e.g., *Whipple and Tucker*, 1999]. If the flood is a point source, then a will be 0 (discharge will not increase downstream) and the m exponent will be negative; that is, incision will decrease downstream as the channel widens, all else being equal. The discharge in the Mandakini during the flood was not exclusively from the breached lake; rainfall during the event was also heavy [*Dobhal et al*., 2013], so during the event discharge still increased downstream, but the m exponent would be depressed. We suggest this as a component of the explanation of the switch to sediment aggradation in the lower reaches of the channel; this will also be enhanced by a high sediment transport load from reworked moraine. It is possible that much of the evacuation of sediment generated during these extreme events is subsequently mobilized out of the system during more moderate monsoonal discharge [e.g., *Hartshorn et al*., 2002].

In addition, the stream power law does not account for channel widening [cf. *Lague*, 2014], and during the event channel widening was widespread. This means that stream power would overpredict erosion rates since it assumes incision will occur over fixed channel geometries. Despite the fact that the chi analysis does not include adjustments for channel widening, areas of channel widening are correlated with area of high M_χ, suggesting that in these areas extreme events should expend energy on channel banks in addition to the channel bed [cf. *Hartshorn et al*., 2002].

A fundamental question in drainage systems is whether it is the extreme geomorphic events that define the long profile of a river channel [*Schumm*, 1973], and if so, how can we use this information to improve hazard mitigation strategies in these settings. In Ladakh, in the lee of the western Himalaya where long-term erosion rates are slow (~0.01 mm yr^{-1}), the impact of extreme monsoonal storms of August 2010 could not be related to the longer-term trajectory of change recorded by the channel profiles [*Hobley et al*., 2010, 2012]. The slowly eroding landscape of Ladakh is clearly transient as much of the river valleys are still occupied by glacial moraine that is dated at circa 100 ka [*Owen et al*., 2006]; these landscapes may be considered to be "buffered" against the extreme events (in a broad sense *Allen* [2005]). The 2013 event in the Mandakini River contrasts with the event in Ladakh: in the Mandakini, $M\chi$ has a spatial distribution that mirrors the spatial distribution of damage during the 2013 event. Thus, the Mandakini River follows the "reactive" model of *Allen* [2005]: its topography, developed over long timescales, appears to relate to the pattern of incision that occurred during a rare, extreme event.

4.2. Conclusion

Mapping of the Mandakini River network using a chi analysis demonstrates high M_χ values in the upper part of the catchment in the hanging wall of the Main Central Thrust. These data suggest that this structure governs the distribution of differential rock uplift during the time of landscape formation in this valley (10^5–10^6 years). Following flash floods during the summer of 2013, the valley was devastated by both channel incision and undercutting of infrastructure, and by burial by coarse boulder debris. Enhanced channel incision occurred along the reaches where M_χ greatest, compared to sediment aggradation (burial) where steepness is less. Because the spatial distribution of topographic modification was consistent with the long river profile as quantified by chi analysis, we suggest that in the frontal Himalaya topographic analysis could provide a valuable first-order approximation of the future impact of extreme flood events in the frontal Himalaya.

Acknowledgments

This work has been funded by University Grant Commission (grant F.5-112/2007 (BRS)), University of Delhi grant (DRCH/R&D/2013-14/4155), U.S. Army Research Office W911NF-13-1-0478, and NERC NE/J012750/1. We acknowledge NASA and METI for the DTM data, which were accessed through the U.S. Geological Survey web link "http://earthexplorer.usgs.gov/."

The Editor thanks two anonymous reviewers for their assistance in evaluating this paper.

References

Allen, P. (2005), Striking a chord, *Nature*, *434*(7036), 961, doi:10.1038/434961a.

Bickle, M. J., N. B. W. Harris, J. M. Bunbury, H. J. Chapman, I. J. Fairchild, and T. Ahmad (2001), Controls on the 87Sr/86Sr ratios of carbonates in the Garhwal Himalaya, Headwaters of the Ganges, *J. Geol.*, *109*(6), 737–753.

Dobhal, D. P., A. K. Gupta, M. Mehta, and D. D. Khandelwal (2013), Kedarnath disaster: Facts and plausible causes, *Current Sci. (00113891)*, *105*(2), 171–174.

Hack, J. T. (1960), Interpretation of erosional topography in humid temperate regions, *Am. J. Sci.*, *258A*, 80–97.

Hancock, G. S., R. S. Anderson, and K. X. Whipple (1998), Beyond power: Bedrock river incision process and form, in *Rivers Over Rock: Fluvial Processes in Bedrock Channels*, vol. 107, edited by K. J. Tinkler and E. E. Wohl, pp. 35–60, AGU, Washington, D. C.

Hartshorn, K., N. Hovius, W. B. Dade, and R. L. Slingerland (2002), Climate-driven bedrock incision in an active mountain belt, *Science*, *297*(5589), 2036–2038, doi:10.1126/science.1075078.

Hobley, D. E. H., H. D. Sinclair, S. M. Mudd, and P. A. Cowie (2011), Field calibration of sediment flux dependent river incision, *J. Geophys. Res.*, *116*, F04017, doi:10.1029/2010JF001935.
Hobley, D. E. J., H. D. Sinclair, and P. A. Cowie (2010), Processes, rates, and time scales of fluvial response in an ancient postglacial landscape of the northwest Indian Himalaya, *Geol. Soc. Am. Bull.*, *122*(9–10), 1569–1584, doi:10.1130/B30048.1.
Hobley, D. E. J., H. D. Sinclair, and S. M. Mudd (2012), Reconstruction of a major storm event from its geomorphic signature: The Ladakh floods, 6 August 2010, *Geology*, *40*(6), 483–486, doi:10.1130/G32935.1.
Hodges, K. V., C. Wobus, K. Ruhl, T. Schildgen, and K. Whipple (2004), Quaternary deformation, river steepening, and heavy precipitation at the front of the Higher Himalayan ranges, *Earth Planet. Sci. Lett.*, *220*(3–4), 379–389, doi:10.1016/S0012-821X(04)00063-9.
Howard, A. D. (1994), A detachment-limited model of drainage basin evolution, *Water Resour. Res.*, *30*, 2261–2285, doi:10.1029/94WR00757.
Kirby, E., and K. X. Whipple (2012), Expression of active tectonics in erosional landscapes, *J. Struct. Geol.*, *44*, 54–75, doi:10.1016/j.jsg.2012.07.009.
Kirby, E., K. Whipple, and N. Harkins (2008), Topography reveals seismic hazard, *Nat. Geosci.*, *1*(8), 485–487, doi:10.1038/ngeo265.
Lague, D. (2014), The stream power river incision model: Evidence, theory and beyond, *Earth Surf. Processes Landforms*, *39*(1), 38–61, doi:10.1002/esp.3462.
Mehta, M., Z. Majeed, D. P. Dobhal, and P. Srivastava (2012), Geomorphological evidences of post-LGM glacial advancements in the Himalaya: A study from Chorabari Glacier, Garhwal Himalaya, India, *J. Earth Syst. Sci.*, *121*(1), 149–163, doi:10.1007/s12040-012-0155-0.
Mudd, S. M., M. Attal, D. T. Milodowski, S. W. D. Grieve, and D. A. Valters (2014), A statistical framework to quantify spatial variation in channel gradients using the integral method of channel profile analysis, *J. Geophys. Res. Earth Surf.*, *119*, 138–152, doi:10.1002/2013JF002981.
Ouimet, W. B., K. X. Whipple, and D. E. Granger (2009), Beyond threshold hillslopes: Channel adjustment to base-level fall in tectonically active mountain ranges, *Geology*, *37*(7), 579–582, doi:10.1130/G30013A.1.
Owen, L. A., M. W. Caffee, K. R. Bovard, R. C. Finkel, and M. C. Sharma (2006), Terrestrial cosmogenic nuclide surface exposure dating of the oldest glacial successions in the Himalayan orogen: Ladakh Range, northern India, *Geol. Soc. Am. Bull.*, *118*(3–4), 383–392, doi:10.1130/B25750.1.
Perron, J. T., and L. Royden (2013), An integral approach to bedrock river profile analysis, *Earth Surf. Processes Landforms*, *38*(6), 570–576, doi:10.1002/esp.3302.
Royden, L. H., M. K. Clark, and K. X. Whipple (2000), Evolution of river elevation profiles by bedrock incision: Analytical solutions for transient river profiles related to changing uplift and precipitation rates, *Eos Trans. AGU*, *81*, Fall Meet. Suppl., Abstract T62F-09.
Royden, L., and J. T. Perron (2013), Solutions of the stream power equation and application to the evolution of river longitudinal profiles, *J. Geophys. Res. Earth Surf.*, *118*, 497–518, doi:10.1002/jgrf.20031.
Scherler, D., B. Bookhagen, and M. R. Strecker (2014), Tectonic control on 10Be-derived erosion rates in the Garhwal Himalaya, India, *J. Geophys. Res. Earth Surf.*, *119*, 1–23, doi:10.1002/2013JF002955.
Schumm, S. A. (1973), Geomorphic thresholds and complex response of drainage systems, *Fluvial Geomorphol.*, *6*, 69–85.
Seeber, L., and V. Gornitz (1983), River profiles along the Himalayan arc as indicators of active tectonics, *Tectonophysics*, *92*(4), 335–367, doi:10.1016/0040-1951(83)90201-9.
Sklar, L., and W. E. Dietrich (1998), River longitudinal profiles and bedrock incision models: Stream power and the influence of sediment supply, in *Rivers Over Rock: Fluvial Processes in Bedrock Channels*, edited by K. J. Tinkler and E. E. Wohl, pp. 237–260, AGU, Washington, D. C.
Snyder, N. P., K. X. Whipple, G. E. Tucker, and D. J. Merritts (2003), Importance of a stochastic distribution of floods and erosion thresholds in the bedrock river incision problem, *J. Geophys. Res.*, *108*(B2), 2117, doi:10.1029/2001JB001655.
Valdiya, K. S., S. K. Paul, T. Chandra, S. S. Bhakuni, and R. C. Upadhyay (1999), Tectonic and lithological characterization of Himadri (Great Himalaya) between Kali and Yamuna rivers, Central Himalaya, *Himalayan Geol.*, *20*(2), 1–17.
Wasson, R. J., Y. P. Sundriyal, S. Chaudhary, M. K. Jaiswal, P. Morthekai, S. P. Sati, and N. Juyal (2013), A 1000-year history of large floods in the Upper Ganga catchment, central Himalaya, India, *Quat. Sci. Rev.*, *77*, 156–166, doi:10.1016/j.quascirev.2013.07.022.
Whipple, K. X., and G. E. Tucker (1999), Dynamics of the stream-power river incision model: Implications for height limits of mountain ranges, landscape response timescales, and research needs, *J. Geophys. Res.*, *104*(B8), 17,661–17,674, doi:10.1029/1999JB900120.
Whipple, K. X., and G. E. Tucker (2002), Implications of sediment-flux-dependent river incision models for landscape evolution, *J. Geophys. Res.*, *107*(B2), 2039, doi:10.1029/2000JB000044.
Willgoose, G., R. L. Bras, and I. Rodriguez-Iturbe (1991), Results from a new model of river basin evolution, *Earth Surf. Processes Landforms*, *16*(3), 237–254, doi:10.1002/esp.3290160305.
Ziegler, A. D., R. J. Wasson, A. Bhardwaj, Y. P. Sundriyal, S. P. Sati, N. Juyal, V. Nautiyal, P. Srivastava, J. Gillen, and U. Saklani (2014), Pilgrims, progress, and the political economy of disaster preparedness—The example of the 2013 Uttarakhand flood and Kedarnath disaster, *Hydrol. Processes*, *28*(24), 5985–5990, doi:10.1002/hyp.10349.